An Orally Available Small-Molecule Inhibitor of c-Met, PF-2341066, Exhibits Cytoreductive Antitumor Efficacy through Antiproliferative and Antiangiogenic Mechanisms

Helen Y. Zou,[1] Qiuhua Li,[1] Joseph H. Lee,[1] Maria E. Arango,[1] Scott R. McDonnell,[1] Shinji Yamazaki,[2] Tatiana B. Koudriakova,[2] Gordon Alton,[3] Jingrong J. Cui,[4] Pei-Pei Kung,[4] Mitchell D. Nambu,[4] Gerrit Los,[1] Steven L. Bender,[5] Barbara Mroczkowski,[6] and James G. Christensen[1]

Departments of [1]Cancer Biology, [2]Pharmacokinetics, Dynamics, and Metabolism, [3]Biochemical Pharmacology, [4]Medicinal Chemistry, [5]Oncology, and [6]Molecular Biology, Pfizer Global Research and Development, La Jolla Laboratories, La Jolla, California

Abstract

The c-Met receptor tyrosine kinase and its ligand, hepatocyte growth factor (HGF), have been implicated in the progression of several human cancers and are attractive therapeutic targets. PF-2341066 was identified as a potent, orally bioavailable, ATP-competitive small-molecule inhibitor of the catalytic activity of c-Met kinase. PF-2341066 was selective for c-Met (and anaplastic lymphoma kinase) compared with a panel of >120 diverse tyrosine and serine-threonine kinases. PF-2341066 potently inhibited c-Met phosphorylation and c-Met–dependent proliferation, migration, or invasion of human tumor cells *in vitro* (IC_{50} values, 5–20 nmol/L). In addition, PF-2341066 potently inhibited HGF-stimulated endothelial cell survival or invasion and serum-stimulated tubulogenesis *in vitro*, suggesting that this agent also exhibits antiangiogenic properties. PF-2341066 showed efficacy at well-tolerated doses, including marked cytoreductive antitumor activity, in several tumor models that expressed activated c-Met. The antitumor efficacy of PF-2341066 was dose dependent and showed a strong correlation to inhibition of c-Met phosphorylation *in vivo*. Near-maximal inhibition of c-Met activity for the full dosing interval was necessary to maximize the efficacy of PF-2341066. Additional mechanism-of-action studies showed dose-dependent inhibition of c-Met–dependent signal transduction, tumor cell proliferation (Ki67), induction of apoptosis (caspase-3), and reduction of microvessel density (CD31). These results indicated that the antitumor activity of PF-2341066 may be mediated by direct effects on tumor cell growth or survival as well as antiangiogenic mechanisms. Collectively, these results show the therapeutic potential of targeting c-Met with selective small-molecule inhibitors for the treatment of human cancers. [Cancer Res 2007;67(9):4408–17]

Introduction

An emerging paradigm in oncology is that robust clinical efficacy can be obtained with inhibitors directed toward oncogenic receptor tyrosine kinases (RTK) that are mutated or otherwise dysregulated in selected advanced tumors (1, 2). Recent examples of successful therapeutic intervention with RTK inhibitors include imatinib in gastrointestinal stromal tumors (GIST) with mutant c-Kit, erlotinib in non–small cell lung cancer (NSCLC) with mutant and/or amplified epidermal growth factor receptor, trastuzumab in breast cancers with amplified/elevated HER-2, and sunitinib targeting the von Hippel-Lindau (VHL)-dependent vascular endothelial growth factor (VEGF) pathway in renal cell carcinoma (RCC; ref. 3). In addition to the aforementioned RTKs, c-Met is one of most frequently genetically altered or otherwise dysregulated RTKs in advanced cancers, implicating it as an attractive therapeutic target (4).

c-Met is the prototypic member of a subfamily of RTKs, which also includes RON. c-Met is structurally distinct from other RTKs and is the only known high-affinity receptor for hepatocyte growth factor (HGF), also known as scatter factor (SF; refs. 5, 6). Binding of HGF to the c-Met extracellular domain results in receptor multimerization and phosphorylation of multiple tyrosine residues at the intracellular region (5, 6). Tyrosine phosphorylation at the c-Met juxtamembrane, catalytic, and cytoplasmic domains regulate the internalization, catalytic activity, and docking of regulatory substrates, respectively (6–9). Activation of c-Met results in the binding and phosphorylation of adaptor proteins, such as growth factor receptor binding protein 2 (Grb2)–associated binding protein 1 (Gab1), Grb2, Src homology and collagen (Shc), and c-Cbl and subsequent activation of signal transducers such as phosphoinositide-3-kinase, Akt, peritoneal lymphocyte-γ (PLC-γ), signal transducers and activators of transcription (STAT), and extracellular signal-regulated kinases 1 and 2 (ERK1 and 2; ref. 10).

c-Met and HGF are expressed in numerous tissues, and their expression is normally confined predominantly to cells of epithelial and mesenchymal origin, respectively (11, 12). c-Met and HGF have been shown to be important in epithelial-mesenchymal interaction and regulation of cell migration, invasion, cell proliferation and survival, angiogenesis, morphogenic differentiation, and organization of three-dimensional tubular structures (e.g., renal tubular cells) during mammalian development and tissue repair and homeostasis (10, 13–16).

Although the controlled regulation of c-Met and HGF have been shown to be important in mammalian development and tissue homeostasis, their dysregulation is implicated in metastatic cancer progression. c-Met and HGF are highly expressed relative to surrounding tissue in numerous cancers, and their expression correlates with poor patient prognosis (10). *c-Met*–activating point mutations in the kinase domain are implicated as the cause of hereditary papillary renal carcinoma and were also detected in sporadic papillary renal carcinoma, lung cancers, head and neck

Note: Supplementary data for this article are available at Cancer Research Online (http://cancerres.aacrjournals.org/).

Requests for reprints: James G. Christensen, Department of Cancer Research, Pfizer Global Research and Development, La Jolla Laboratories, 10724 Science Center Drive, La Jolla, CA 92121. Phone: 858-638-6336; Fax: 858-526-4120; E-mail: james.christensen@pfizer.com.

doi:10.1158/0008-5472.CAN-06-4443

cancers, childhood hepatocellular carcinoma, and gastric cancer (17–22). Furthermore, amplification of the *c-Met* gene locus was detected in patients with gastric, metastatic colorectal cancer, and esophageal adenocarcinoma (23, 24). Cell lines engineered to express high levels of c-Met and HGF (autocrine loop) or mutant c-Met displayed a proliferative, motogenic, and/or invasive phenotype and grew as metastatic tumors in nude mice (25–29). Furthermore, HGF and c-Met have been implicated in the regulation of tumor angiogenesis through the direct proangiogenic properties of HGF or through the regulation of secretion of angiogenic factors, including VEGFA, interleukin-8 (IL-8), and thrombospondin-1 (30–33).

Although a number of inhibitors of the c-Met pathway have been identified, including HGF kringle variants/NK4, decoy receptors, or HGF neutralizing antibodies, the therapeutic utility of these approaches still requires clinical validation (4). Previously described small-molecule inhibitors of c-Met (e.g., SU11274 or PHA-665752) have been limited to *in vitro* studies or brief *in vivo* studies and were not viable clinical agents due to poor pharmaceutical properties and oral bioavailability (34). The present studies describe the identification and characterization of PF-2341066, an orally available ATP-competitive and selective small-molecule inhibitor of c-Met. PF-2341066 potently inhibited c-Met phosphorylation and signal transduction, as well as c-Met–dependent oncogenic phenotypes of tumor cells and endothelial cells *in vitro* and showed antitumor efficacy in tumor models at well-tolerated doses *in vivo*. Antitumor mechanism-of-action studies indicated that the antitumor activity of PF-2341066 may be mediated by both direct effects on tumor cell growth or survival, as well as antiangiogenic mechanisms.

Materials and Methods

Compound

PF-2341066 [(*R*)-3-[1-(2,6-dichloro-3-fluoro-phenyl)-ethoxy]-5-(1-piperidin-4-yl-1*H*-pyrazol-4-yl)-pyridin-2-ylamine; Supplementary Fig. S1] was synthesized at Pfizer, La Jolla Laboratories.

Biochemical Kinase Assays

c-Met catalytic activity was quantitated using a continuous-coupled spectrophotometric assay in which the time-dependent production of ADP by c-Met was determined by analysis of the rate of consumption of NADH. NADH consumption was measured by a decrease in absorbance at 340 nm by spectrophotometry at designated time points. To determine K_i values, PF-2341066 was introduced into test wells at various concentrations in the presence of assay reagents and incubated for 10 min at 37°C. The assay was initiated by the addition of the c-Met enzyme.

Cells

Unless otherwise mentioned, cells were acquired from the American Type Culture Collection. GTL-16 gastric carcinoma cells and T47D breast carcinoma cells engineered to express human wild-type c-Met or its mutant variant c-Met Y1235D were donated by Dr. Paolo Comoglio or Dr. Mariaflavia DiRenzo (both from the University Torino Medical School, Candiolo, Italy), respectively. All cells were cultured in recommended media and serum concentration, and unless otherwise indicated, cell culture reagents were obtained from Life Technologies, Inc. Cells were maintained at 37°C in a humidified atmosphere with 5% to 10% CO_2 and maintained using standard cell culture techniques.

Antibodies and Growth Factors

Anti–total human c-Met was acquired from Zymed/Invitrogen. Anti-CD31 and anti–phospho-tyrosine (PY-20) were acquired from Santa Cruz Biotechnology. Anti-mouse c-Met was acquired from R&D Systems. Anti–phospho–c-Met; anti–total and phospho-Gab1; anti–total and phospho-Akt; anti–total and phospho-ERK1 and 2; and STAT5 were acquired from Cell Signaling Technologies. Antibodies used in immunohistochemistry studies included anti–phospho-c-Met (Biosource International/Invitrogen) and anti-Ki67 (DakoCytomation). Growth factors used in cell assays were each acquired from R&D Systems.

Cell Assays

All experiments were done under standard conditions (37°C and 5% CO_2). IC_{50} values were calculated by concentration-response curve fitting using a Microsoft Excel–based four-parameter method.

Cellular kinase phosphorylation ELISA assays. Cells were seeded in 96-well plates in media supplemented with 10% fetal bovine serum (FBS) and transferred to serum-free media [with 0.04% bovine serum albumin (BSA)] after 24 h. In experiments investigating ligand-dependent RTK phosphorylation, corresponding growth factors were added for up to 20 min. After incubation of cells with PF-2341066 for 1 h and/or appropriate ligands for the designated times, cells were washed once with HBSS supplemented with 1 mmol/L Na_3VO_4, and protein lysates were generated from cells. Subsequently, phosphorylation of selected protein kinases was assessed by a sandwich ELISA method using specific capture antibodies used to coat 96-well plates and a detection antibody specific for phosphorylated tyrosine residues. Antibody-coated plates were (*a*) incubated in the presence of protein lysates at 4°C overnight; (*b*) washed seven times in 1% Tween 20 in PBS; (*c*) incubated in a horseradish peroxidase–conjugated anti–total-phosphotyrosine (PY-20) antibody (1:500) for 30 min; (*d*) washed seven times again; (*e*) incubated in 3,3′,5,5′-tetramethyl benzidine peroxidase substrate (Bio-Rad) to initiate a colorimetric reaction that was stopped by adding 0.09 N H_2SO_4; and (*f*) measured for absorbance in 450 nm using a spectrophotometer.

Cell proliferation/survival assays. Tumor cells were seeded in 96-well plates at low density in media supplemented with 10% FBS (growth media) and transferred to serum-free media (0% FBS and 0.04% BSA) after 24 h. Appropriate controls or designated concentrations of PF-2341066 were added to each well, and cells were incubated for 24 to 72 h. Human umbilical vascular endothelial cells (HUVEC) (passage 3) were seeded in 96-well plates in EGM2 media for 5 to 6 h at >20,000 cells per well and transferred to serum-free media (Cell Applications) overnight. The following day, appropriate controls or designated concentrations of PF-2341066 were added to each well, and after 1 h incubation, HGF was added to designated wells at 100 ng/mL. A 3-(4,5-dimethylthiazol-2-yl)-2,5-diphenyltetrazolium bromide assay (Promega) was done to determine the relative tumor cell or HUVEC numbers.

Tumor cell migration and Matrigel invasion assays. NCI-H441 cell migration and Matrigel invasion were determined using a modified commercially available kit (BD Biosciences). Briefly, cells in log growth phase were trypsinized and suspended in serum-free media (with 0.04% BSA) at a density of 400,000 cells/mL. Designated control or treated suspended cells (0.5 mL) were added to each migration or invasion chamber (i.e., plate inserts) and incubated at 37°C for 22 h. In addition, 25 ng/mL HGF (0.75 mL) was added to the lower well of each companion plate to attract cells from migration or invasion chamber plate inserts at the top of the companion plate. Cells that invaded or migrated to the lower wells were then fixed and stained with 4′,6-diamidino-2-phenylindole for 15 min at 37°C and washed twice with TBS, and the number of invading cells was quantitated using Image-Pro Plus software over a composite of five microscopic images (Media Cybernetics).

HUVEC Matrigel invasion assay. ACEA electrosensing 96-well plates were coated with 50 μL of 0.001% fibronectin and 100 ng/mL HGF in PBS and incubated at 37°C for 1 h and then at 4°C for 30 min. After washing each plate with PBS at 4°C, Matrigel (BD Biosciences) diluted 1:40 in starvation media (Cell Applications), supplemented with HGF (100 ng/mL) and/or different concentrations of PF-2341066, was added (50 μL) to designated wells and allowed to solidify at 37°C for 2 h. HUVEC were subsequently collected in starvation media at 60,000 cells/mL and treated with 100 ng/mL HGF and/or designated concentrations of PF-2341066 for 30 min at 37°C, and 100 μL of suspended cells were transferred to the top of

the Matrigel layer in the coated ACEA plate. The ACEA plate was connected to the ACEA Device Station at 37°C, and HUVEC that invaded through Matrigel were monitored in real time by an ACEA Sensor Analyzer for 48 h and quantitated using ACEA RT-CES Integrated Software.

Madin-Darby canine kidney cell scattering assay. Madin-Darby canine kidney cell (MDCK) scattering assays were done as described previously (34).

Human dermal microvascular endothelial cells vascular sprouting assay. Approximately 500 human dermal microvascular endothelial cells (HMVEC) (Clonetics) were added to EGM-2 medium containing 0.24% methylcellulose and transferred to U-bottomed 96-well plates to form spheroids overnight. Spheroids were supplemented with 2 mg/mL fibrinogen and 4% FBS with vehicle or designated concentrations of PF-2341066 in 48-well thrombin-coated plates and incubated in EGM-2 containing 4% FBS at 37°C and 5% CO_2. Endothelial tube formation was assessed, and images were captured on day 7 with an inverted microscope and Olympus BX60 digital camera.

Apoptosis assay. GTL-16 cells were seeded in 96-well plates at 40,000 cells per well. Designated concentrations of PF-2341066 or vehicle were added to the wells in serum-free media, and cells were incubated in 37°C and 5% CO_2 for 48 h. The ssDNA Apoptosis ELISA kit (Chemicon) was used to detect apoptosis.

In vivo Studies

Animals. Female or male *nu/nu* mice (5–8 weeks old) were obtained from Charles River. Animals were maintained under clean room conditions in sterile filter top cages with Alpha-Dri bedding and housed on high-efficiency particulate air–filtered ventilated racks. Animals received sterile rodent chow and water ad libitum. All of the procedures were conducted in accordance with the Institute for Laboratory Animal Research Guide for the Care and Use of Laboratory Animals and with Pfizer Animal Care and Use Committee guidelines.

S.c. xenograft models in athymic mice. Cells were harvested, pelleted by centrifugation at 450 × *g* for 5 to 10 min, and resuspended in sterile serum-free medium supplemented with 30% to 50% Matrigel (BD Biosciences). Cells ($2–5 \times 10^6$ in 100 μL) were implanted s.c. into the hind-flank region of each mouse and allowed to grow to the designated size before the administration of compound. For studies with NCI-H441, DLD-1, and MDA-MB-231 xenografts, MRC-5 cells were added to tumor cells at a 2:1 ratio (tumor cells/MRC-5) before implantation as a source of bioactive human HGF.

c-Met pharmacodynamic and signal transduction studies. Athymic mice bearing xenografts (300–800 mm^3)were given PF-2341066 in water by oral gavage at designated dose levels. At designated times following PF-2341066 administration, mice were humanely euthanized, and tumors were resected. Tumors were snap frozen and pulverized using a liquid nitrogen-cooled cryomortar and pestle, protein lysates were generated, and protein concentrations were determined using a BSA assay (Pierce). The level of total and phosphorylated protein was determined using a capture ELISA or immunoprecipitation-immunoblotting method.

Efficacy studies. Daily treatment with PF-2341066 given in water by oral gavage was initiated when tumors were 100 to 600 mm^3 in volume. Tumor volume was determined by measurement with electronic Vernier calipers, and tumor volume was calculated as the product of its length × $width^2$ × 0.4. Tumor volume was expressed on indicated days as the median tumor volume ± SE indicated for groups of mice. Percent (%) inhibition values were measured on the final day of study for drug-treated compared with vehicle-treated mice and are calculated as $100 \times \{1-[(Treated_{Final\ day} - Treated_{Day\ 1})/(Control_{Final\ day} - Control_{Day\ 1})]\}$. Tumor regression values were determined by calculating the ratio of median tumor volumes at the time when treatment was initiated to median tumor volume on the final day of study for a given treatment group. Significant differences between the treated versus the control groups ($P \leq 0.001$) were determined using one-way ANOVA.

Immunohistochemistry. Tumor specimens were fixed in 10% buffered formalin for 24 h before being transferred to 70% ethanol. Tumor samples were subsequently paraffin-embedded, and 4 μmol/L sections were cut and baked onto microscope slides. Slides were incubated with the primary antibodies then secondary antibodies and visualized using a colorimetric method (DAB kit; DAO Envision-HARP). All of the immunostained sections were counterstained using hematoxylin. An automated Ventana Discovery XT Staining Module (Ventana Medical Systems) was used to conduct histologic staining. Stained sections were analyzed using an Olympus microscope, and quantitative analysis of section staining was done using the ACIS system (Automated Cellular Imaging, Clarient).

Results

PF-2341066 potently inhibited the catalytic activity of c-Met and its oncogenic variants *in vitro*. PF-2341066 (Supplementary Fig. S1) was selected for further characterization based on screens designed to identify inhibitors of c-Met. PF-2341066 was shown to be a potent ATP-competitive inhibitor of recombinant, human c-Met kinase activity with a mean K_i of 4 nmol/L. In cell-based assays, PF-2341066 inhibited HGF-stimulated or constitutive total tyrosine phosphorylation of wild-type c-Met, with a mean IC_{50} value of 11 nmol/L across a panel of human tumor and endothelial cell lines (Supplementary Table S1). PF-2341066 showed similar potency against c-Met phosphorylation in mIMCD3 mouse (IC_{50}, 5 nmol/L) or MDCK canine (IC_{50}, 20 nmol/L) epithelial cells.

c-Met–activating mutations have been identified in several human cancers and provide a strong rationale for clinical proof of concept studies. To address differences in potency against mutant variants of c-Met, PF-2341066 was evaluated for its ability to inhibit c-Met phosphorylation across a panel of cell lines expressing c-Met mutations (Supplementary Table S1). In these studies, PF-2341066 exhibited improved or similar activity against NIH3T3 cells engineered to express c-Met ATP-binding site mutants V1092I (IC_{50}, 19 nmol/L) or H1094R (IC_{50}, 2 nmol/L) or the P-loop mutant M1250T (IC_{50}, 15 nmol/L) compared with NIH3T3 cells expressing wild-type receptor (IC_{50}, 13 nmol/L). In contrast, a marked shift in potency was observed against cells engineered to express c-Met activation loop mutants Y1230C (IC_{50}, 127 nmol/L) and Y1235D (IC_{50}, 92 nmol/L) compared with wild-type receptor. PF-2341066 also potently inhibited c-Met phosphorylation in NCI-H69 (IC_{50}, 13 nmol/L) and HOP92 (IC_{50}, 16 nmol/L) cells, which express the endogenous c-Met variants R988C and T1010I, respectively.

Kinase selectivity of PF-2341066. PF-2341066 was evaluated in >120 biochemical kinase assays done at Upstate, Inc., or Pfizer and was determined to be more than 100-fold selective for c-Met compared with the majority (>90%) of kinases evaluated (data not shown). In cell-based assays to follow up initial biochemical data, PF-2341066 was >1,000-fold selective for the VEGFR2 and PDGFRβ RTKs, >250-fold selective for IRK and Lck, and ~40- to 60-fold selective for Tie2, TrkA, and TrkB, all compared with c-Met (Supplementary Table S1). PF-2341066 was 20- to 30-fold selective for RON and Axl RTKs (Supplementary Table S1), however; pharmacologically relevant inhibitory activity (proposed as IC_{90} for 24 h) is unlikely to be achieved at efficacious doses of PF-2341066 based on assessment of *in vivo* pharmacodynamics for other RTK targets (data not shown). In contrast, PF-2341066 showed a near-equivalent IC_{50} value (24 nmol/L) against the nucleophosmin (NPM)-anaplastic lymphoma kinase (ALK) oncogenic fusion variant of the ALK RTK expressed by the KARPAS299 human anaplastic large cell lymphoma (ALCL) cell line. These data indicate that the pharmacologic activity of PF-2341066 is likely mediated by the inhibition of c-Met and ALK RTKs and their oncogenic variants. The pharmacologic properties of PF-02341066

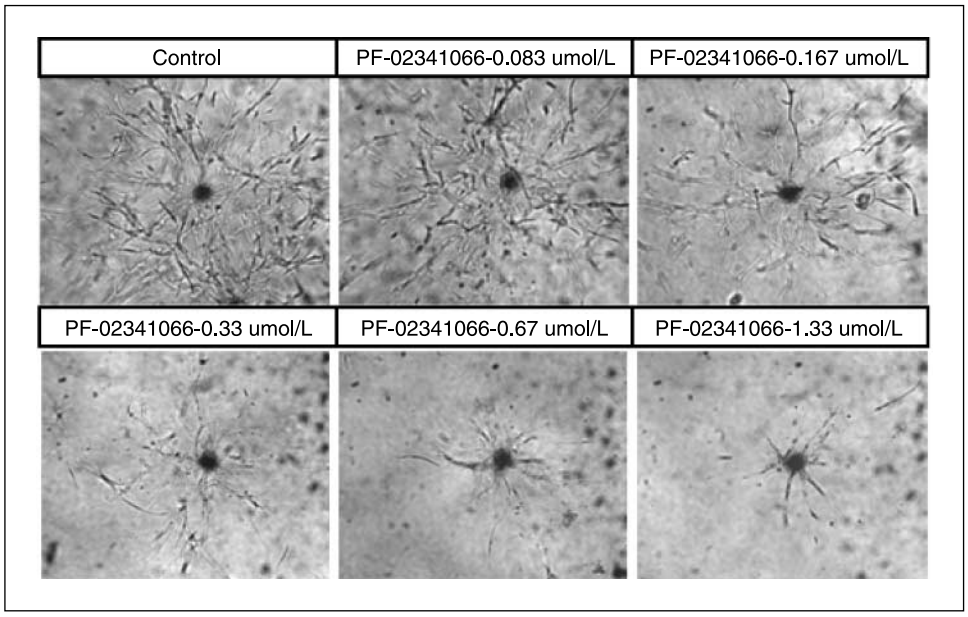

Figure 1. PF-2341066 inhibited HMVEC endothelial cell tubulogenesis *in vitro*. HMVEC cells were plated as spheroids in a collagen-fibrin matrix, and subsequent endothelial cell tubulogenesis was observed within 7 d following initial plating. PF-2341066 was added to spheroid cultures at day 7 at the indicated concentrations, and the effect on the number and length of endothelial cell tubules was visually assessed.

in models of NPM-ALK–positive lymphoma will be described elsewhere.[7]

PF-2341066 inhibited c-Met–dependent neoplastic phenotypes of cancer cells and angiogenic phenotypes of endothelial cells *in vitro*. Because c-Met is implicated in a variety of tumor cell and tumor endothelial cell functions, PF-2341066 was evaluated in a series of cell-based functional assays. PF-2341066 inhibited human GTL-16 gastric carcinoma cell growth (IC_{50}, 9.7 nmol/L), induced apoptosis in GTL-16 cells (IC_{50}, 8.4 nmol/L), inhibited HGF-stimulated human NCI-H441 lung carcinoma cell migration and invasion (Supplementary Fig. S2, IC_{50}s of 11 and 6.1 nmol/L, respectively), and inhibited MDCK cell scattering (IC_{50}, 16 nmol/L; Supplementary Table S2).

In studies done using HUVEC, PF-2341066 inhibited HGF-stimulated c-Met phosphorylation (IC_{50}, 11 nmol/L), cell survival (IC_{50}, 14 nmol/L), and Matrigel invasion (IC_{50}, 35 nmol/L; Supplementary Table S2). In addition, PF-2341066 inhibited serum-stimulated HMVEC branching tubulogenesis (formation of vascular tubes) in fibrin gels (Fig. 1). The strong correlation of IC_{50} values for inhibition of c-Met phosphorylation and c-Met–dependent phenotypes suggests that PF-2341066 pharmacologic activity in these assays is mediated by the inhibition of c-Met.

Dose-dependent relationship of c-Met phosphorylation and tumor growth inhibition by PF-2341066 in c-Met–dependent tumor xenograft models. Due to the robust expression of constitutively active c-Met and dependence of c-Met for tumor cell growth and survival, GTL-16 tumors were used to evaluate the relationship of c-Met target inhibition to tumor growth inhibition by PF-2341066 *in vivo*. To evaluate c-Met inhibition by PF-2341066, GTL-16 tumors were harvested at several time points following p.o. administration of PF-2341066 over a range of doses, and c-Met phosphorylation in tumors was quantitated by ELISA. In these studies, PF-2341066 showed the following as shown in Fig. 2 (*A* and *B*):

- At 50 mg/kg/day, 100% tumor growth inhibition correlated with complete inhibition of c-Met phosphorylation in GTL-16 tumors sustained for 24 h. At dose levels of >50 mg/kg/day, no further improvement of tumor growth inhibition was observed (data not shown).
- At 12.5 mg/kg/day, 60% tumor growth inhibition correlated with 80% to 90% inhibition of c-Met phosphorylation at 1 to 8 h, which decreased to 50% to 60% inhibition by 16 to 24 h.
- At 6.25 mg/kg/day, nonsignificant trend toward tumor growth inhibition correlated with 30% to 50% inhibition of c-Met phosphorylation at 1 to 8 h with full recovery by 16 h.

The following conclusions were apparent from these analyses: (*a*) complete inhibition of c-Met activity for 24 h is consistent with complete inhibition of tumor growth [50 mg/kg; 100% tumor growth inhibition (TGI)]; (*b*) potent inhibition of c-Met activity for only a portion of the schedule is consistent with suboptimal efficacy (12.5 mg/kg; 60% TGI); (*c*) inability to achieve >50% inhibition of c-Met activity (3.125, 6.25 mg/kg) is consistent with lack of significant TGI (Fig. 2*A* and *B*). In addition, a similar dose-dependent effect of PF-2341066 on tumor growth and c-Met phosphorylation (at 4 h) was observed using the U87MG glioblastoma xenograft model (Fig. 2*C* and *D*). Collectively, these studies suggest that near-complete inhibition of c-Met phosphorylation (>90% inhibition) for the duration of the administration schedule is necessary to maximize therapeutic benefit.

Antitumor efficacy of PF-2341066 in c-Met–dependent human xenograft models. Additional studies were done at optimal dose levels of PF-2341066 to assess its efficacy in human tumor xenograft models representative of cancer indications in which dysregulation of c-Met is implicated. Due to the lack of paracrine activation of human c-Met expressed in tumors by mouse HGF expressed by mouse mesenchymal cells, human xenograft models exhibiting constitutive c-Met activity were used as follows: (*a*) the GTL-16 human gastric carcinoma or Caki-1 RCC models that expresses elevated levels of constitutively active c-Met; (*b*) the U87MG human glioblastoma or PC-3 human prostate carcinoma model that expresses both HGF and c-Met comprising an autocrine loop; or (*c*) coimplantation of human tumor cells

[7] J.G. Christensen, H.Y. Zou, M.E. Arango, et al. A novel inhibitor of anaplastic lymphoma kinase (ALK) and c-Met demonstrates complete regression in an experimental model of anaplastic large cell lymphoma through antiproliferative and proapoptotic mechanisms, submitted for publication.

(e.g., NCI-H441 NSCLC, DLD-1 colon cancer, MDA-MB-231 breast cancer) with human MRC5 fibroblasts to supply a source of bioactive human HGF to enable species-specific paracrine activation of c-Met.

In the GTL-16 model, PF-2341066 showed the ability to cause marked regression of large established tumors (>600 mm^3) in both the 50 and 75 mg/kg/day treatment cohorts, with a 60% decrease in mean tumor volume over the 43-day administration schedule (Fig. 3*A*). In the GTL-16 study, each tumor decreased in volume during the treatment cycle (50 or 75 mg/kg/day), with 9 of 14 mice exhibiting a >30% decrease in tumor mass and one animal exhibiting no evidence of tumor even after cessation of treatment for 10 days (Fig. 3*A*). In an additional study, PF-2341066 showed the ability to completely suppress GTL-16 tumor growth for >3 months, with only 1 of 12 mice exhibiting a significant increase in tumor growth over the 3-month treatment schedule at 50 mg/kg/day (data not shown).

In the NCI-H441 NSCLC model, a 43% decrease in mean tumor volume was observed at 50 mg/kg/day during the 38-day PF-2341066 administration cycle (Fig. 3*B*). In the NCI-H441 study, each tumor decreased in mass during the treatment cycle at 50 mg/kg/day, with 3 of 11 mice exhibiting a >30% decrease in tumor mass, and 3 animals with no evidence of tumor at the end of the treatment cycle. In the Caki-1 RCC model, a 53% decrease in mean tumor volume was observed associated with decreased volume of each tumor by at least 30% at 50 mg/kg/day during the 33-day PF-2341066 administration cycle (Fig. 3*C*).

PF-2341066 also showed near-complete inhibition of the growth of established tumors at 50 mg/kg/day in the U87MG glioblastoma or PC-3 prostate carcinoma xenograft models, with 97% or 84% inhibition on the final study day, respectively (Figs. 2*D* and 3*D*). In contrast, PF-2341066 p.o. given at 50 mg/kg/day did not significantly inhibit tumor growth in the MDA-MB-231 breast carcinoma model, or the DLD-1 colon carcinoma model (data not shown). In each study, PF-2341066 was well tolerated at 50 mg/kg/day for as long as 3 months or at 200 mg/kg/day for as long as 1 month, with no weight loss or evidence of overt toxicity or histopathologic findings. Collective *in vivo* experiments showed robust dose-dependent antitumor efficacy of PF-2341066 at well-tolerated dose levels in a variety of diverse tumor models, which correlated with the degree of inhibition of c-Met phosphorylation in tumor tissue.

PF-2341066 mechanism of action in c-Met–dependent tumor models. PF-2341066 was also evaluated for its effect on tumor mitotic index (Ki67) and apoptosis (activated caspase-3) using immunohistochemical (IHC) methods. A significant 4-fold decrease in Ki67 levels by study day 4 was observed at 25 and 50 mg/kg/day PF-2341066 in the GTL-16 (Fig. 4*A–C*) and U87MG (data not shown) models indicating a correlation with maximum antitumor efficacy. In addition, the evaluation of the 50 mg/kg dose over a time course indicated that the inhibition of mitogenesis was markedly more potent at days 3 and 4, suggesting that extended target inhibition maximizes this potentially cell cycle–dependent effect (Fig. 4*D*). Furthermore, a qualitative induction of activated caspase-3 at 25 and 50 mg/kg/day was observed in the GTL-16 model and at 50 mg/kg/day in the U87MG model (Supplementary Fig. S3). Similar to the modulation of Ki67, the increased apoptosis was dose dependent and correlated with the degree of antitumor efficacy of PF-2341066 (data not shown).

To evaluate the potential antiangiogenic mechanism of this compound *in vivo*, PF-2341066 was evaluated for time- and dose-dependent modulation of microvessel density (MVD) assessed by immunostaining for CD31 (platelet endothelial cell adhesion

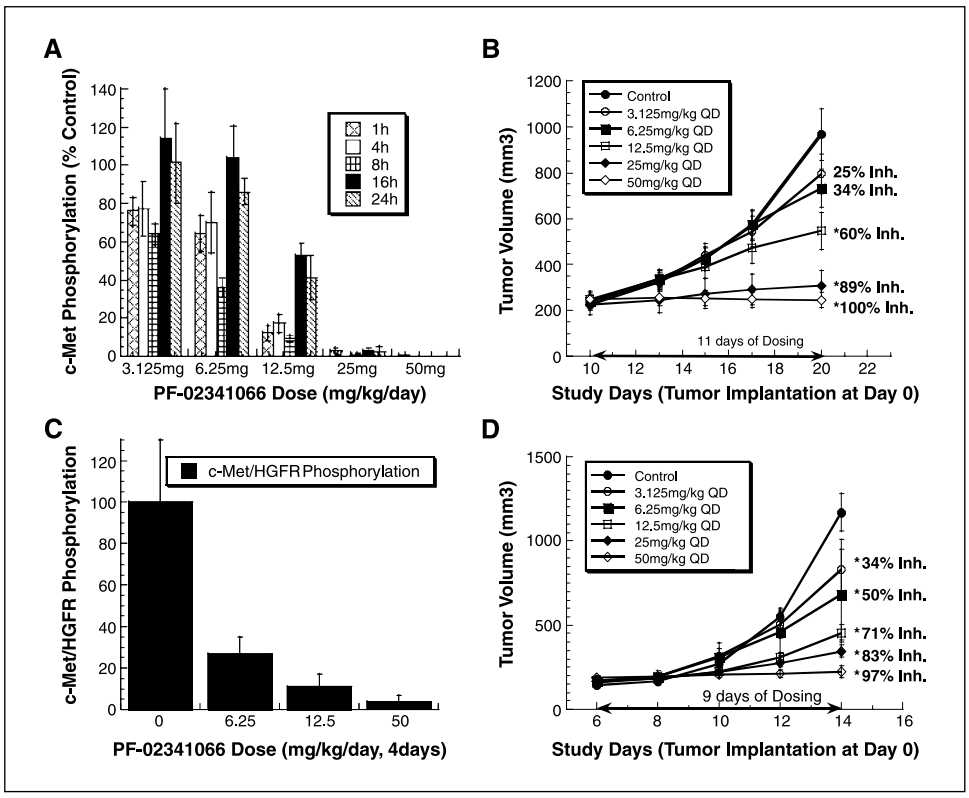

Figure 2. Inhibition of c-Met phosphorylation (*A*) and tumor growth (*B*) by PF-2341066 in GTL-16 xenograft model. Athymic mice bearing established GTL-16 (250 mm^3; *A* and *B*) or U87MG (180 mm^3; *C* and *D*) tumors were given PF-2341066 p.o. at the indicated dose or vehicle alone over the designated treatment schedule. For studies investigating inhibition of c-Met phosphorylation (*A* or *C*), mice were humanely euthanized at designated time points postadministration, tumors were resected and frozen, and phosphorylation in vehicle and treated groups was quantitated by ELISA. Inhibition of kinase target phosphorylation by PF-2341066 in tumors was calculated as % inhibition = 100 − [(mean OD treated/mean OD untreated) × 100]. For studies investigating tumor growth inhibition (*B* or *D*), tumor volume was measured using Vernier calipers on the indicated days with the median tumor volume ± SE indicated for groups of 15 mice. Percent tumor growth inhibition values were measured on the final day of study for drug-treated compared with vehicle-treated mice and were calculated as $100 \times \{1 - [(Treated_{Day\ 20} - Treated_{Day\ 10})/(Control_{Day\ 20} - Control_{Day\ 10})]\}$. *, $P \leq 0.001$, median tumor volumes are significantly less in the treated versus the control group as determined using one-way ANOVA.

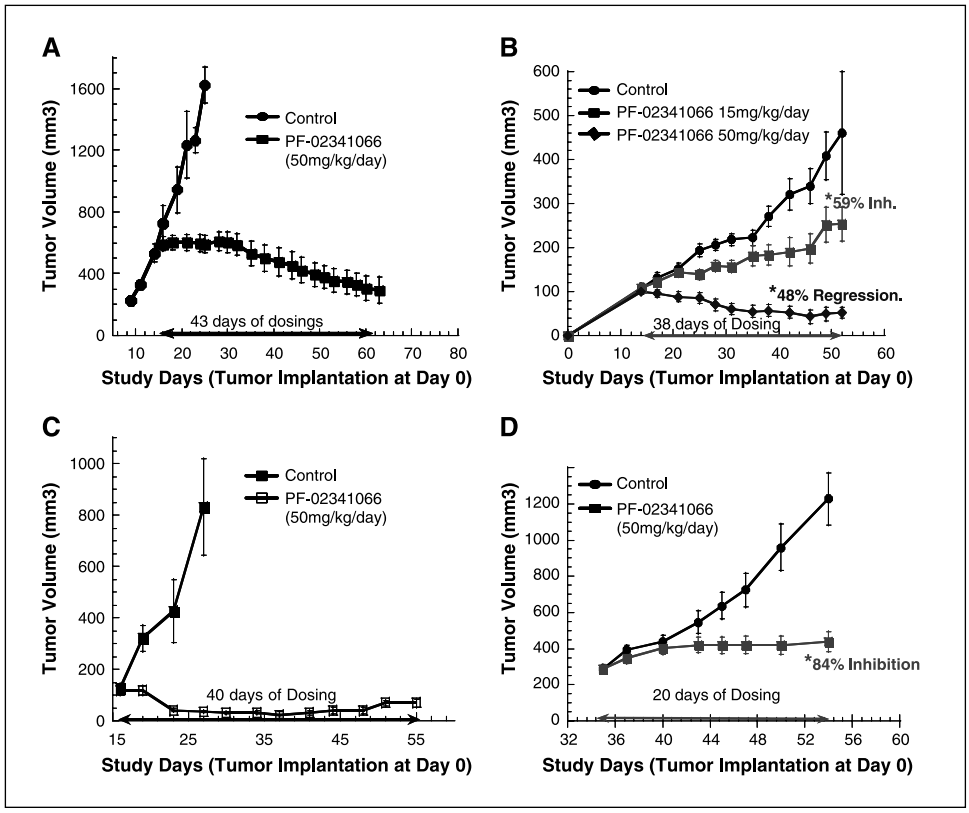

Figure 3. Antitumor efficacy of PF-2341066 in the GTL-16 gastric (*A*), NCI-H441 NSCL (*B*), Caki-1 renal (*C*), or PC-3 prostate (*D*) carcinoma xenograft models. Athymic mice bearing established GTL-16 (600 mm^3; *A*), NCI-H441 (100 mm^3; *B*), Caki-1 (100 mm^3; *C*), or PC-3 (250 mm^3; *D*) tumors were given PF-2341066 p.o. at the indicated dose levels or vehicle alone over the designated treatment schedule. Tumor volume was measured using Vernier calipers on the indicated days with the median tumor volume ± SE indicated for groups of 10 to 15 mice. *, $P \leq 0.001$, median tumor volumes are significantly less in the treated versus the control group as determined using one-way ANOVA.

molecule 1). A significant dose-dependent reduction of CD31–positive endothelial cells was observed at 12.5, 25, and 50 mg/kg/day in GTL-16 tumors, indicating that inhibition of MVD showed a dose-dependent correlation to antitumor efficacy (Fig. 5*A* and *B*). At the 50 mg/kg/day dose level, PF-02340166 showed a significant 70% reduction of CD31-positive microvessels at study day 11 (Fig. 5*A* and *B*). In contrast, the effect on MVD was less apparent in the short-term time course study, suggesting that reduction of MVD requires longer term administration. In contrast to the GTL-16 model, only slight effects on MVD were observed in the U87MG model, suggesting that this potential antiangiogenic mechanism depends on tumor type.

c-Met and HGF have also been shown to regulate the secretion of proangiogenic factors, including VEGFA and IL-8 by tumor cells (32, 33). Therefore, the effect of PF-2341066 on VEGFA and IL-8 plasma levels was assessed to elucidate whether the effects on MVD observed following the administration of PF-2341066 were due to direct or indirect effects on tumor vessels. In these studies, PF-2341066 showed a significant dose-dependent reduction of human VEGFA and IL-8 plasma levels in both the GTL-16 and U87MG models (U87MG, Fig. 5*C*). Human VEGFA and IL-8 were not present in the plasma of non–tumor-bearing mice, indicating that the source of these plasma proteins was the tumor tissue (data not shown). A significant acute reduction of IL-8 or VEGFA plasma levels was observed after 1 or 2 days of PF-2341066 administration, respectively, in mice with size-matched tumor xenografts, indicating that observed effects were not due to differences in tumor burden (Fig. 5*D*).

Effect of PF-2341066 on signal transduction pathways in tumors *in vivo*. To investigate the effect of PF-2341066 on critical c-Met–dependent signal transduction events, immunoblot analysis of phosphorylation of molecules that regulate c-Met signal transduction was done using tumor tissue. In these studies, marked inhibition of phosphorylated c-Met, Akt, Erk, PLCλ1, and STAT5 levels was observed in GTL-16 tumors following p.o. administration of PF-2341066 (Fig. 6). Inhibition of these signaling events was dose dependent and was observed at pharmacologically relevant PF-2341066 dose levels, which correlated with the inhibition of c-Met phosphorylation, antitumor efficacy, and other mechanistic end points *in vivo* (Fig. 6).

Discussion

In the present studies, we describe a novel orally available inhibitor of c-Met and the consequences of inhibiting this RTK target in a variety of functional assays and tumor models. This prototype small molecule, PF-2341066, was identified as a potent ATP-competitive inhibitor of c-Met kinase, which inhibited c-Met phosphorylation across a panel of cell lines. The similar inhibitory activity against c-Met human and mouse epithelial cells has implications for interpreting potential antiangiogenic activity and safety profile of PF-2341066 during studies in tumor xenograft models in mice.

The clinical success with RTK inhibitors such as imatinib and erlotinib in patient populations exhibiting mutated RTK targets indicates that treatment of neoplasms with activating *Met* mutations comprises a viable clinical strategy for PF-2341066. PF-2341066 inhibited a variety of diverse mutant variants of c-Met in cellular assays, including those located at the ATP binding pocket (V1092I and H1094R), P-loop (M1250T), and juxtamembrane domain (R988C and T1010I). In contrast, PF-2341066 was less potent against the Y1230C and Y1235D mutant variants of c-Met located near the kinase domain activation loop. These data indicate that PF-2341066 activity is dependent on the location of

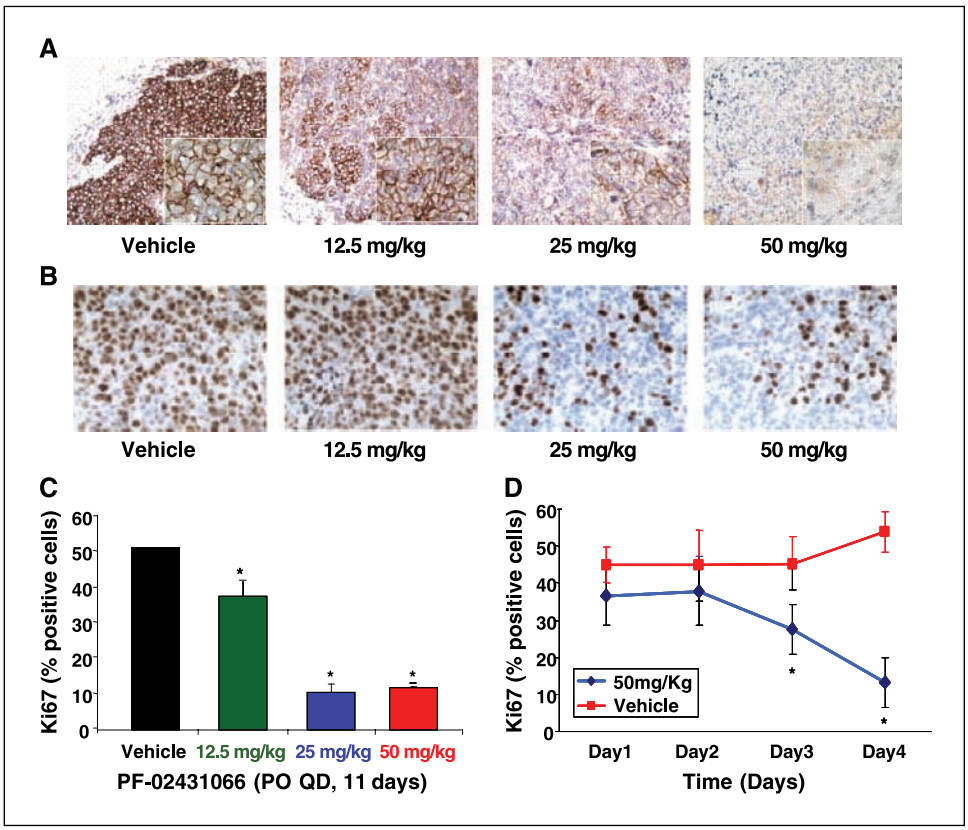

Figure 4. Dose-dependent inhibition of c-Met phosphorylation (*A*) or tumor cell proliferation (*B–D*) by PF-2341066 in tumor xenografts *in vivo*. Immunohistochemical evaluation of c-Met phosphorylation (*A*) or Ki67 (*B* and *C*) expression at indicated dose levels was determined in GTL-16 tumors on study day 4. Immunohistochemical evaluation of Ki67 expression was also assessed at days 1 to 4 at 50 mg/kg/day q.d. (*D*) in GTL-16 tumors. For all studies, athymic mice bearing established GTL-16 or U87MG xenografts were p.o. given vehicle or PF-2341066 at the indicated dose levels q.d. At designated study days at 4 h postadministration of PF-2341066, mice were humanely euthanized, and tumors were resected and fixed in 10% neutral buffered formalin for 24 h, and then placed in 70% ethanol. Fixed tumors were embedded in paraffin, cut into 4-mm sections, and immunostained for c-Met or Ki67 as described in Materials and Methods. Slides were visually assessed for expression and distribution of c-Met or Ki67 by light microscopy, and quantitative analysis of Ki67 expression was determined using an ACIS system as described in Materials and Methods. *, $P \leq 0.01$, significant difference from the control group as determined using one-way ANOVA.

the mutation in the active site, which has unique implications in molecular modeling of c-Met inhibitory activity. These data indicate that selected mutations identified in papillary renal carcinoma, head and neck, and lung cancers are effectively inhibited by PF-2341066, and that particular mutations (e.g., activation loop) should be taken into account during patient selection (17, 19, 20, 22).

Evaluation of PF-2341066 across a structurally diverse cross-section of nearly 25% of all known tyrosine and serine-threonine kinases (35) indicated that it exhibited a high degree of selectivity at pharmacologically relevant concentrations. The exception to this was ALK, which was inhibited at pharmacologically relevant (24 nmol/L) concentrations by PF-2341066 in lymphoma cell lines expressing the NPM-ALK oncogenic fusion protein. Similar to BCR-Abl in chronic myelogenous leukemia, available literature indicates that ALK fusion proteins are a key disease driver of ALCL (36). In the present studies, disease models selected for study of c-Met–dependent pharmacology generally do not express ALK, suggesting that the pharmacologic activity of PF-2341066 is likely due to the inhibition of c-Met. However, due to the expression of wild-type ALK in selected endothelial cell populations, the relevance of ALK in mediating the pharmacologic activity of PF-2341066 cannot be discounted (37, 38).

The identification of PF-2341066 as a potent and selective inhibitor of c-Met provided some unique opportunities to investigate the pharmacologic consequences of c-Met inhibition. With the strong correlation between IC_{50} values required for inhibition of c-Met phosphorylation and tumor or endothelial cell phenotypes, the present studies suggest that the pharmacologic effects of PF-2341066 are due to the inhibition of c-Met. These collective phenotypic data indicate that potential anticancer effects of PF-2341066 may range from (*a*) direct effects on tumor cell growth and survival to (*b*) antimetastatic properties through inhibition of tumor cell migration and invasion and may include (*c*) potential anitangiogenic activity mediated through direct effects on the ability of endothelial cells to form functional vasculature. In addition, the strong correlation of inhibition of c-Met and c-Met–dependent phenotypes by PF-2341066 indicates that c-Met phosphorylation should function as a useful pharmacodynamic biomarker of inhibition of c-Met–mediated function in tumors. To this effect, studies relating pharmacodynamics to efficacy indicated that near-complete inhibition of c-Met phosphorylation (>90% inhibition) for the duration of the administration schedule is necessary to maximize antitumor efficacy of PF-2341066. These data indicate that maintaining a sufficient degree of c-Met inhibition in patients will be critical in maximizing the therapeutic potential of this agent, and that a strategy to measure c-Met phosphorylation in patient tumor biopsies or surrogate tissue is warranted.

Following the identification of optimal dose levels of PF-2341066, studies were initiated to determine the sensitivity a variety of tumor models to this agent. The models selected for these studies represented different mechanisms by which c-Met has been reported to be activated in human tumors, including (*a*) paracrine activation by HGF expressed in tumor-associated mesenchymal tissue, (*b*) autocrine expression of both c-Met and HGF by tumor cells, and (*c*) expression of constitutively active c-Met due to increased expression or amplification of its gene locus. In these studies, PF-2341066 showed cytoreductive antitumor activity in models expressing high levels of constitutively activated c-Met, including GTL-16 gastric or Caki-1 renal carcinoma. These data indicate that gastric carcinoma patients with amplified c-Met or

renal patients with high levels of constitutively activated c-Met may comprise clinical populations that exhibit higher probability of objective response to PF-2341066. This concept is further supported by chemosensitivity of a panel of gastric cancer cell lines exhibiting amplified c-Met to a putative selective inhibitor of c-Met (39) and by increased expression and activation of c-Met in renal carcinoma cells devoid of functional VHL (40). Similarly, U87MG glioblastoma or PC-3 prostate carcinoma models in which tumor cells express both HGF and c-Met each exhibited a robust response to PF-2341066, supporting the concept that tumor types that exhibit autocrine production of c-Met and HGF may also be candidates for clinical studies. In contrast, although a robust response of the NCI-H441 NSCLC paracrine model to PF-23410666 was observed, other paracrine c-Met–expressing models such as MDA-MB-231 breast and DLD-1 colon carcinoma did not respond. These data suggest that response of populations in which wild-type c-Met is expressed in the absence of the constitutively active RTK or autocrine HGF may exhibit a heterogeneous response to c-Met–directed therapy. These data indicate that further study of molecular determinants sensitivity to c-Met–directed therapy is warranted. Chemosensitivity studies with selective c-Met inhibitors across a panel of human tumor cell lines expressing wild-type c-Met indicate that the response to these agents is heterogeneous and associated with selected molecular characteristics (4).

In addition to understanding molecular determinants of chemosensitivity, a basic understanding of the mechanism of action of PF-2341066 antitumor activity should also support a robust clinical strategy. As described above, PF-2341066 showed a direct effect on tumor cell growth and survival end points *in vitro* and dose-dependent inhibition of cell proliferation and induction apoptosis in tumors *in vivo*. Therefore, one mechanism of PF-2341066 is likely mediated via direct effects on tumor cell mitogenesis and apoptosis in tumor types in which dysregulation of c-Met is implicated in altered tumor cell growth regulation. In addition, Ki67 and activated casapase-3 were modulated in models that responded to PF-2341066 but were unaffected in those that did not (data not shown), indicating that these end points may represent markers of antitumor efficacy.

In the present studies, PF-2341066 also showed the ability to inhibit HGF-stimulated endothelial cell survival and migration, to inhibit endothelial cell tubulogenesis, and to reduce MVD in the GTL-16 model. In addition to their reported direct role in regulating endothelial cell function, c-Met and HGF are also implicated in the regulation of secretion of angiogenic factors by

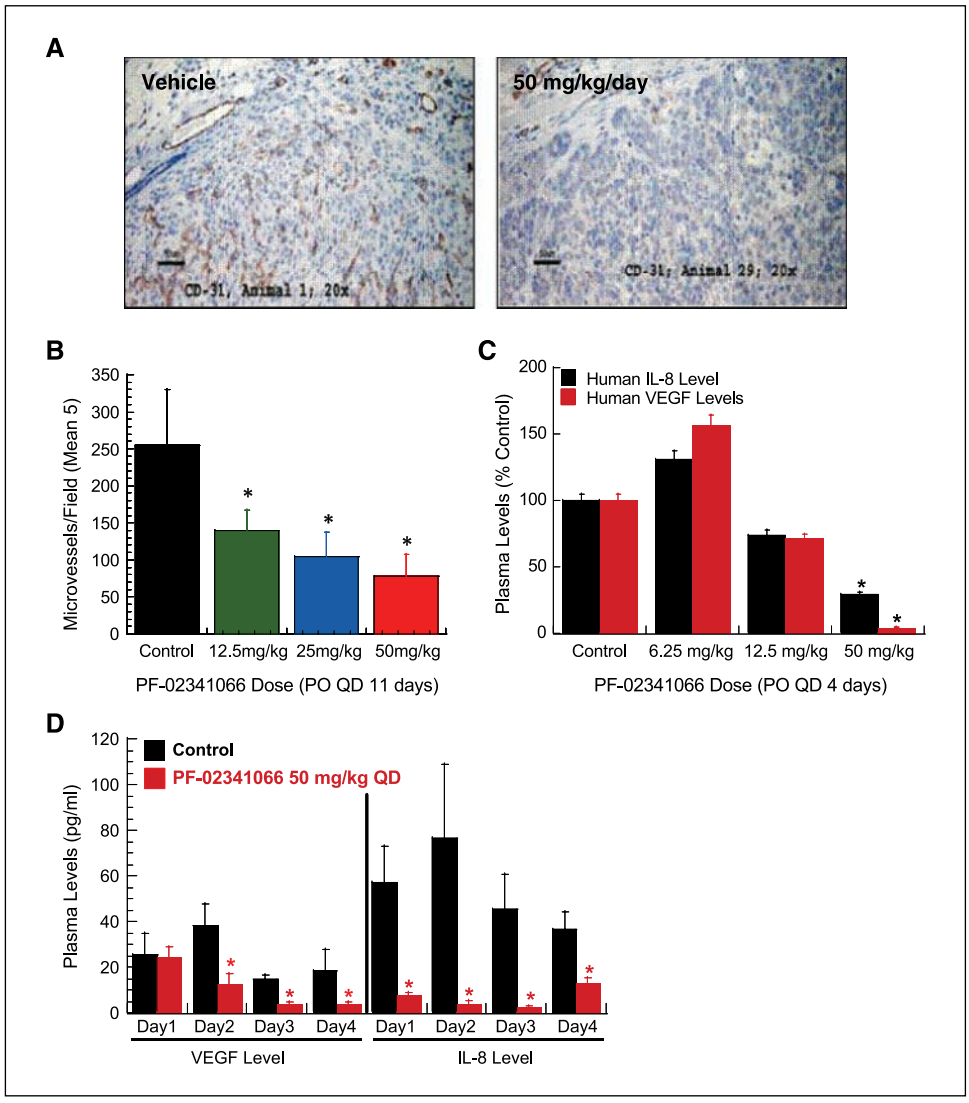

Figure 5. Effect of PF-2341066 on tumor MVD (*A* and *B*) or secretion of proangiogenic factors (*C* and *D*) in tumor xenografts *in vivo*. Athymic mice bearing established GTL-16 or U87MG xenografts were given PF-2341066 p.o. at the indicated dose levels or vehicle. For (*A*) and (*B*), on study day 11 at 4 h postadministration of PF-2341066, resected tumors were frozen/fixed in Tissue Tek OCT compound. Cryogenic sections were cut and immunostained for CD31 and counterstained with hematoxylin. Slides were visually assessed by light microscopy (*A*), and quantitative analysis of CD31-positive endothelial cells was done using ACIS System (*B*) as described in Materials and Methods. For (*C*) and (*D*), heparinized plasma was collected from the left ventricle of mice bearing U87MG (*C*) of GTL-16 (*D*) xenografts at designated study days at 4 h postadministration of PF-2341066. Plasma levels of human VEGFA or IL-8 were determined at each study day using commercially available ELISA kits from R&D Systems. *, $P \leq 0.05$, significant difference from the control group as determined using one-way ANOVA.

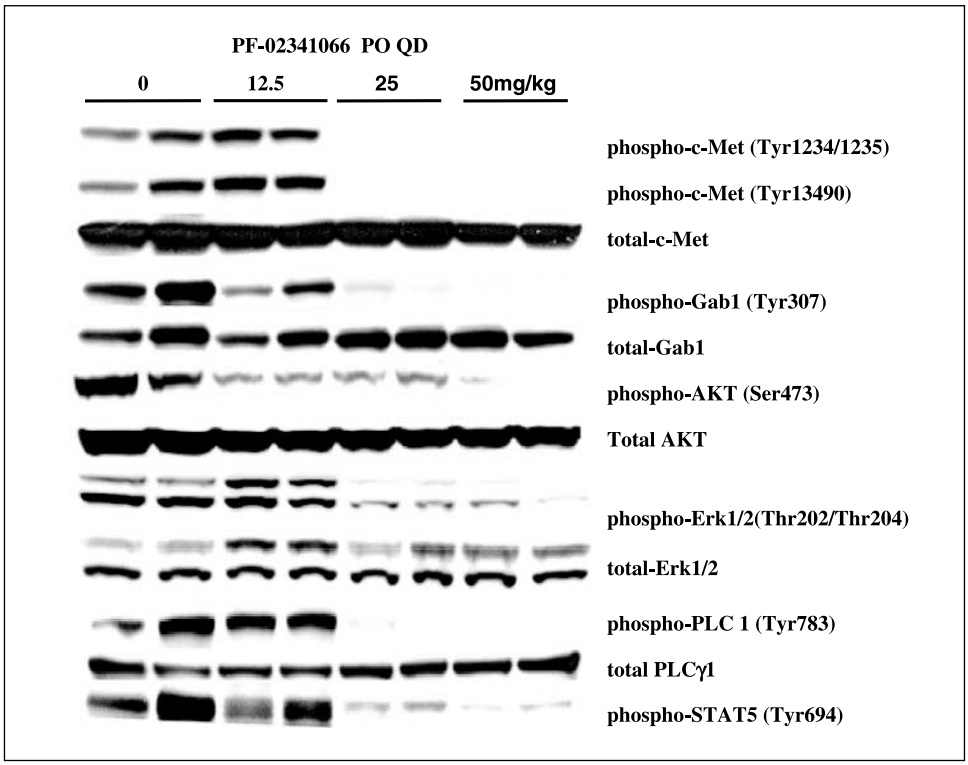

Figure 6. Dose-dependent inhibition of c-Met phosphorylation and downstream signaling pathways in GTL-16 tumors by PF-2341066. Athymic mice bearing established GTL-16 xenografts were given PF-2341066 p.o. at the indicated dose or vehicle 11 d. Mice were humanely euthanized on study day 11 at 4 h postadministration of PF-2341066, and tumors were resected, snap-frozen, and pulverized. Protein lysates were generated from tumor samples and resolved by SDS-PAGE, and immunoblotting was done for each protein or phosphoprotein of interest using specific antibodies as described in Materials and Methods.

epithelial and tumor cells. In the present studies, PF-2341066 showed a robust modulation of VEGF and IL-8 in the GTL-16 and U87MG tumor models that correlated with its antitumor activity. Together, these data suggest that antiangiogenic activity observed with PF-2341066 may be mediated by direct or indirect mechanisms. If the antiangiogenic activity of PF-2341066 is dependent on the functional expression of c-Met by tumor cells, this will have implications in terms of the breadth of spectrum of antiangiogenic activity across tumor types. The absence of evidence of PF-2341066 antiangiogenic activity in the U87MG model and the absence of efficacy in the MDA-MB-231 and DLD-1 models suggest that the antiangiogenic activity of this agent is dependent on factors that are not common to all tumor types. Therefore, although PF-2341066 showed antiangiogenic properties in selected assays and models, it is not evident that this agent will exhibit broad spectrum antitumor activity through an antiangiogenic activity similar to VEGF pathway antagonists (41).

In summary, these studies illustrate the pharmacologic effects of PF-2341066 on a variety of pro-oncogenic tumor cell phenotypes, tumor models, and molecular mediators of cancer progression. The broad antitumor efficacy and good safety profile of this molecule suggest its potential as a novel agent for treatment of a variety of cancers. The variety of different responses to PF-2341066 observed in tumor cells and endothelial cells illustrates that this compound is likely to exert its antitumor effects through multiple distinct mechanisms. In addition, collective results indicate that the role of c-Met in the progression of cancers may differ depending on the cell lineage of origin and genetic context of a given tumor cell. The diverse role of c-Met in different tumor types as a regulator of tumor growth, survival, or metastasis will be a critical issue in the clinical development of c-Met inhibitors, monitoring of patient response, and design of clinical studies.

Acknowledgments

Received 12/4/2006; revised 1/27/2007; accepted 2/15/2007.

The costs of publication of this article were defrayed in part by the payment of page charges. This article must therefore be hereby marked *advertisement* in accordance with 18 U.S.C. Section 1734 solely to indicate this fact.

We thank Dr. Paolo Comoglio and Dr. Maria Flavia DiRenzo for the original supply of GTL-16 cells and of T47D cells (expressing c-Met Y1235D or wild type), respectively.

References

1. Blume-Jensen P, Hunter T. Oncogenic kinase signalling. Nature 2001;411:355–65.
2. Schlessinger J. Cell signaling by receptor tyrosine kinases. Cell 2003;103:211–25.
3. Baselga J. Targeting tyrosine kinases in cancer: the second wave. Science 2006;312:1175–8.
4. Christensen J, Burrows J, Salgia R. c-Met as a target for human cancer and characterization of inhibitors for therapeutic intervention. Cancer Lett 2005;225:1–25.
5. Bottaro DP, Rubin JS, Faletto DL, et al. Identification of the hepatocyte growth factor receptor as the c-met proto-oncogene product. Science 1991;251:802–4.
6. Naldini L, Vigna E, Narsimhan RP, et al. Hepatocyte growth factor (HGF) stimulates the tyrosine kinase activity of the receptor encoded by the proto-oncogene c-MET. Oncogene 1991;6:501–4.
7. Fournier TM, Lamorte L, Maroun CR, et al. Cbl-transforming variants trigger a cascade of molecular alterations that lead to epithelial mesenchymal conversion. Mol Biol Cell 2000;11:3397–410.
8. Ponzetto C, Bardelli A, Zhen Z, et al. A multifunctional docking site mediates signaling and transformation by the hepatocyte growth factor/scatter factor receptor family. Cell 1994;77:261–71.
9. Rodrigues GA, Park M. Autophosphorylation modulates the kinase activity and oncogenic potential of the Met receptor tyrosine kinase. Oncogene 1994;9:2019–27.
10. Birchmeier C, Birchmeier W, Gherardi E, Vande Woude GF. Met, metastasis, motility and more. Nat Rev Mol Cell Biol 2003;4:915–25.
11. Di Renzo MF, Narsimhan RP, Olivero M, et al.

Expression of the Met/HGF receptor in normal and neoplastic human tissues. Oncogene 1991;6:1997–2003.
12. Sonnenberg E, Weidner KM, Birchmeier C. Expression of the met-receptor and its ligand, HGF-SF during mouse embryogenesis. EXS 1993;65:381–94.
13. Comoglio PM, Trusolino L. Invasive growth: from development to metastasis [comment]. J Clin Invest 2002;109:857–62.
14. Bladt F, Riethmacher D, Isenmann S, Aguzzi A, Birchmeier C. Essential role for the c-met receptor in the migration of myogenic precursor cells into the limb bud. Nature 1995;376:768–71.
15. Schmidt C, Bladt F, Goedecke S, et al. Scatter factor/hepatocyte growth factor is essential for liver development. Nature 1995;373:699–702.
16. Tsarfaty I, Rong S, Resau JH, et al. The Met proto-oncogene mesenchymal to epithelial cell conversion. Science 1994;263:98–101.
17. Di Renzo MF, Olivero M, Martone T, et al. Somatic mutations of the MET oncogene are selected during metastatic spread of human HNSC carcinomas. Oncogene 2000;19:1547–55.
18. Lee JH, Han SU, Cho H, et al. A novel germ line juxtamembrane Met mutation in human gastric cancer. Oncogene 2000;19:4947–53.
19. Ma PC, Jagdeesh S, Jagadeeswaran R, et al. c-MET expression/activation, functions, and mutations in non–small cell lung cancer. Proc Amer Assoc Cancer Res 2004;44:1875.
20. Ma PC, Kijima T, Maulik G, et al. c-MET mutational analysis in small cell lung cancer: novel juxtamembrane domain mutations regulating cytoskeletal functions. Cancer Res 2003;63:6272–81.
21. Park WS, Dong SM, Kim SY, et al. Somatic mutations in the kinase domain of the Met/hepatocyte growth factor receptor gene in childhood hepatocellular carcinomas. Cancer Res 1999;59:307–10.
22. Schmidt L, Duh FM, Chen F, et al. Germline and somatic mutations in the tyrosine kinase domain of the MET proto-oncogene in papillary renal carcinomas. Nat Genet 1997;16:68–73.
23. Di Renzo MF, Olivero M, Giacomini A, et al. Overexpression and amplification of the met/HGF receptor gene during the progression of colorectal cancer. Clin Cancer Res 1995;1:147–54.
24. Kuniyasu H, Yasui W, Kitadai Y, et al. Frequent amplification of the c-met gene in scirrhous type stomach cancer. Biochem Biophys Res Commun 1992; 189:227–32.
25. Bellusci S, Moens G, Gaudino G, et al. Creation of an hepatocyte growth factor/scatter factor autocrine loop in carcinoma cells induces invasive properties associated with increased tumorigenicity. Oncogene 1994;9:1091–9.
26. Jeffers M, Rong S, Anver M, Vande Woude GF. Autocrine hepatocyte growth factor/scatter factor-Met signaling induces transformation and the invasive/metastastic phenotype in C127 cells. Oncogene 1996; 13:853–6.
27. Jeffers M, Schmidt L, Nakaigawa N, et al. Activating mutations for the met tyrosine kinase receptor in human cancer. Proc Natl Acad Sci U S A 1997;94: 11445–50.
28. Rong S, Bodescot M, Blair D, et al. Tumorigenicity of the met proto-oncogene and the gene for hepatocyte growth factor. Mol Cell Biol 1992;12:5152–8.
29. Rong S, Segal S, Anver M, Resau JH, Vande Woude GF. Invasiveness and metastasis of NIH 3T3 cells induced by Met-hepatocyte growth factor/scatter factor autocrine stimulation. Proc Natl Acad Sci U S A 1994;91: 4731–5.
30. Rosen EM, Goldberg ID. Regulation of angiogenesis by scatter factor. EXS 1997;79:193–208.
31. Rosen EM, Grant DS, Kleinman HK, et al. Scatter factor (hepatocyte growth factor) is a potent angiogenesis factor *in vivo*. Symp Soc Exp Biol 1993; 47:227–34.
32. Zhang YW, Su Y, Volpert OV, Vande Woude GF. Hepatocyte growth factor/scatter factor mediates angiogenesis through positive VEGF and negative thrombospondin 1 regulation. Proc Natl Acad Sci U S A 2003; 100:12718–23.
33. Gille J, Khalik M, Konig V, Kaufmann R. Hepatocyte growth factor/scatter factor (HGF/SF) induces vascular permeability factor (VPF/VEGF) expression by cultured keratinocytes. J Invest Dermatol 1998;111: 1160–5.
34. Christensen JG, Schreck R, Burrows J, et al. A selective small molecule inhibitor of c-Met kinase inhibits c-Met–dependent phenotypes *in vitro* and exhibits cytoreductive antitumor activity *in vivo*. Cancer Res 2003;63:7345–55.
35. Manning G, Whyte DB, Martinez R, Hunter T, Sudarsanam S. The protein kinase complement of the human genome. Science 2002;298:1912–34.
36. Drexler HG, Gignac SM, von Wasielewski R, Werner M, Dirks WG. Pathobiology of NPM-ALK and variant fusion genes in anaplastic large cell lymphoma and other lymphomas. Leukemia 2000;14:1533–59.
37. Choudhuri R, Zhang HT, Donnini S, Ziche M, Bicknell R. An angiogenic role for the neurokines midkine and pleiotrophin in tumorigenesis. Cancer Res 1997;57:1814–9.
38. Stoica GE, Kuo A, Powers C, et al. Midkine binds to anaplastic lymphoma kinase (ALK) and acts as a growth factor for different cell types. J Biol Chem 2002;277: 35990–8.
39. Smolen GA, Sordella R, Muir B, et al. Amplification of MET may identify a subset of cancers with extreme sensitivity to the selective tyrosine kinase inhibitor PHA-665752. Proc Natl Acad Sci U S A 2005;103:2316–21.
40. Oh RR, Park JY, Lee JH, et al. Expression of HGF/SF and Met protein is associated with genetic alterations of VHL gene in primary renal cell carcinomas. APMIS 2002; 110:229–38.
41. Kerbel RS. Antiangiogenic therapy: a universal chemosensitization strategy for cancer? Science 2006; 312:1171–5.